PROPAGATION OF ULTRA WIDE-BAND SIGNALS IN LOSSY DISPERSIVE MEDIA

Yosef Pinhasi, Asher Yahalom, Sergey Petnev
Department of Electrical and Electronic Engineering
Ariel University Center of Samaria
P.O. Box 3, Ariel 40700, ISRAEL

ABSTRACT

Development of a channel model for continuous frequencies enables the analysis of communications in an ultra wide band wireless network in indoor environment including a single transmitting and a single receiving antenna. In this work we will describe a model taking into account multiple reflections which are a consequence of the room in which both transmitter and receiver are localized including wall, ceiling and floor reflections. Moreover, our model enables the analysis of a communication channel between adjacent and distant rooms, in those cases we take into account the wide band signal propagation through separating walls. The model developed is in the frequency domain and thus allows analyzing dispersive effects in transmission and reflection of ultra short pulses in UWB communications from building materials which the room is made of in accordance with their complex dielectric coefficients. For this purpose a library of material characteristics of various materials (concrete, reinforced concrete, plaster, wood, blocks, glass, stone and more) in the standard frequency domain for wireless networks was assembled. One of the important phenomena for UWB communications which our research has revealed is the in-wall multiple reflections resulting in echoes of the narrow pulse transmitted. Our model takes into account antenna polarization and beam shape, the effect of those traits are clearly distinguishable.
Space-frequency theory of the propagation of an ultra-wide band radiation in dielectric media is presented. The transfer function of a slab of material is derived in the frequency domain, considering polarization losses via a complex permittivity. It is shown that absorptive and dispersive effects play a role in the transmission and reflection coefficients of the electromagnetic incident field. The theory is applicable in the analysis of broadband communication links operating in wireless local or personal area networks. In an indoor scenario, the construction material of the walls attenuates the propagating waves in a dispersive manner, causing amplitude and phase distortions in the transmitted signal.

1. INTRODUCTION

During recent years, wireless communications has become an issue of extensive research. The Wireless Local Area Network (WLAN) is used to communicate between nodes up to few tens of mega bits per second. The conventional designated frequencies for WLAN systems are within the Industrial Scientific and Medical (ISM) 2.4-2.4835 band and the Unlicensed National Information Infrastructure (UNII) 5.15-5.35GHz and 5.725-5.825GHz bands.

The Wireless Personal Area Network (WPAN) system is designed to provide short-range, high-speed multi-media data services to terminals located in rooms or office spaces. Two continuous blocks of frequencies were allocated for indoor short-range networks, the band of 3.1-10GHz and 59-64 GHz one [1]. The unique capabilities of the ultra wideband (UWB) technique may promise reliable links between nodes located in different rooms. It was suggested to integrate the 5GHz and the 60 GHz bands to enable operation in indoor and outdoor environments [2].

One of the principal challenges in realizing high data rate, wireless communication links in indoor or indoor-outdoor scenarios are the phenomena arising during the

propagation of electromagnetic waves inside a construction [3]-[4]. Transmission of UWB signals is dominated by the frequency dependent dielectric properties of the material composing the propagation medium. It is well recognized that walls introduce attenuation. However dispersive effects are also expected due to their slab structure, creating a dielectric resonator.

In this paper we present a space-frequency model for broadband links, considering the complex dielectric properties of the materials of the building walls. Based on the approach, a numerical model will be developed enabling examination of the absorptive and dispersive effects on propagation of radio waves through the walls at the super- and extremely- high frequencies.

2. PRESENTATION OF ELECTROMAGNETIC WAVES IN THE FREQUENCY DOMAIN

The electromagnetic field in the time domain is described by the space-time electric $E(r,t)$ and magnetic $H(r,t)$ signal vectors. r stands for the $(\mathrm{x},\mathrm{y},\mathrm{z})$ coordinates, where (x,y) are the transverse coordinates and z is the axis of propagation. The Fourier transform of the electric field is defined by:

(1)
$$\mathbf{E}(r,f)=\int_{-\infty}^{+\infty}E(r,t)\cdot e^{-j2\pi ft}dt$$

where f *denotes* the frequency. Similar expression is defined for the Fourier transform $\mathbf{H}(r,f)$ of the magnetic field. Since the electromagnetic signal is real (i.e. $E^{*}(r,t)=E(r,t)$), its Fourier transform satisfies $\mathbf{E}^{*}(r,f)=\mathbf{E}(r,-f)$. Analytic representation of the signal is given by the complex expression [5]:

(2)
$$\tilde{E}(r,t)=E(r,t)+j\hat{E}(r,t)$$

where

(3)
$$\hat{E}(r,t)=\frac{1}{\pi t}*E(r,t)=\int_{-\infty}^{+\infty}\frac{E(r,t')}{\pi(t-t')}dt'$$

is the Hilbert transform of $E(r,t)$. Fourier transformation of the analytic representation (2) results in a 'phasor-like' function $\tilde{\mathbf{E}}(r,f)$ defined in the positive frequency domain and related to the Fourier transform by:

(4)
$$\tilde{\mathbf{E}}(r,f)=\begin{cases}2\mathbf{E}(r,f) & f>0\\ 0 & f<0\end{cases}$$

The Fourier transform can be decomposed in terms of the phasor like functions according to:

(5) $$\mathbf{E}(r,f)=\frac{1}{2}\tilde{\mathbf{E}}(r,f)+\frac{1}{2}\tilde{\mathbf{E}}^{*}(r,-f)$$

and the inverse Fourier transform is then:

(6) $$E(r,t)=\int_{-\infty}^{+\infty}\mathbf{E}(r,f)\cdot e^{+j2\pi ft}df=\mathrm{Re}\int_{0}^{\infty}\tilde{\mathbf{E}}(r,f)\cdot e^{+j2\pi ft}df$$

3. ELECTROMAGNETIC WAVES IN DIELECTRIC MEDIA

Propagation of electromagnetic waves in a medium can be viewed as a transformation through a linear system. A plane wave propagating in a (homogeneous) medium is given in the frequency domain by:

(7) $$\tilde{\mathbf{E}}_{out}(f)=\tilde{\mathbf{E}}_{in}(f)\cdot e^{-jk(f)d}$$

Here, $k(f)=2\pi f\sqrt{\mu\varepsilon}$ is a frequency dependent propagation factor, where ε and μ are the permittivity and the permeability of the material composing the medium, respectively. In a dielectric medium the permeability is equal to that of the vacuum $\mu=\mu_0$ and the permittivity is given by $\varepsilon(f)=\varepsilon_r(f)\cdot\varepsilon_0$. The polarization in dielectric materials with a finite conductivity is accounted via a complex relative permittivity:

(8) $$\varepsilon_r(f)=\varepsilon'(f)-j\varepsilon''(f)$$

The relative permittivity is a frequency dependent quantity with a real part $\varepsilon'(f)\geq 1$ and an imaginary part $\varepsilon''(f)=\frac{\sigma}{2\pi f\cdot\varepsilon_0}$ where σ is the conductivity of the material. The ratio between the imaginary and real parts is known as the 'loss tangent' $tg[\delta(f)]=\frac{\varepsilon''(f)}{\varepsilon'(f)}=\frac{\sigma}{2\pi f\cdot\varepsilon_0\cdot\varepsilon'(f)}$. The propagation factor can be presented by:

(9) $$k(f)=\frac{2\pi f}{c}\sqrt{\varepsilon_r(f)}=\frac{2\pi f}{c/\sqrt{\varepsilon'(f)}}\cdot\sqrt{1-j\cdot tg[\delta(f)]}$$

where $c=\frac{1}{\sqrt{\mu_0\varepsilon_0}}$ is the speed of light. The propagating wave can be written as:

(10) $$\mathbf{E}_{out}(f)=\mathbf{E}_{in}(f)\cdot e^{-[\alpha(f)+j\beta(f)]d}$$

where $\alpha(f) = -\mathrm{Im}\{k(f)\}$ is the attenuation coefficient and $\beta(f) = \mathrm{Re}\{k(f)\}$ is the wave number of the propagating wave. The real and imaginary parts are determined from:

(11)
$$\alpha^2(f) - \beta^2(f) = -\left(\frac{2\pi f}{c}\right)^2 \varepsilon'(f)$$
$$2\alpha(f)\beta(f) = \left(\frac{2\pi f}{c}\right)^2 \varepsilon'(f) tg(\delta)$$

Solution of the set (11) results in [6]:

(12)
$$\alpha(f) = \frac{2\pi f}{c}\sqrt{\frac{\varepsilon'(f)}{2}\left\{\sqrt{1+tg^2[\delta(f)]}-1\right\}}$$
$$\beta(f) = \frac{2\pi f}{c}\sqrt{\frac{\varepsilon'(f)}{2}\left\{\sqrt{1+tg^2[\delta(f)]}+1\right\}}$$

The dielectric properties of several building materials are summarized in Table 1 Table 2 for the frequencies 5GHz and 60 GHz respectively.

Table 1: Dielectric properties of building materials measured at 5 GHz.

MATERIALS	**5 GHz**			
	Relative Permittivity			
	Real	Imaginary	Conductivity	Tangent loss
	ε'	**ε"**	**σ**	**Tan(δ)**
Brick (made of chalk, with holes)	4.12	0.16	4.45E-02	3.88E-02
Brick (without holes)	3.3	0.01	2.78E-03	3.03E-03
Brick wall	3.56	0.34	9.46E-02	9.55E-02
Concrete (one year)	5.5	0.18	5.01E-02	3.27E-02
Concrete (40 years)	4.6	0.24	6.68E-02	5.22E-02
Wood (a)	2.05	0.296	8.23E-02	1.44E-01
Wood (b)	1.65	0.235	6.54E-02	1.42E-01
Plasterboard	2.02	0.05328	1.48E-02	2.64E-02
Chipboard	2.88	0.4879	1.36E-01	1.70E-01
Glass	5.98	1.0764	2.99E-01	1.80E-01

Table 2: Dielectric properties of building materials measured at 60 GHz.

MATERIALS	60 GHz			
	Relative Permittivity			
	Real	Imaginary	Conductivity	Tan loss
	ε'	**ε''**	**σ**	**Tan(δ)**
Brick (made of chalk, with holes)	3.95	0.073	2.44E-01	1.85E-02
Brick (without holes)	3.26	0	0.00E+00	0.00E+00
Concrete (one year)	6.4954	0.4284	1.43E+00	6.60E-02
Concrete (50 mm)	11.47	0.29593	9.88E-01	2.58E-02
Aerated Concrete	2.26	0.1017	3.39E-01	4.50E-02
Aerated Concrete (50mm)	3.66	0.12481	4.17E-01	3.41E-02
wood	1.5	0.09	3.00E-01	6.00E-02
wood	1.64	1.115	3.72E+00	6.80E-01
Plain wood (19mm, 1 layer)	2.0687	0.41388	1.38E+00	2.01E-01
Plain wood (19mm, 2 layer)	1.9515	0.3683	1.23E+00	1.89E-01
Plasterboard (5mm, 1 layer)	2.4845	0.06211	2.07E-01	2.50E-02
Plasterboard (5mm, 2 layer)	1.8427	0	0.00E+00	0.00E+00
Plasterboard (5mm air gap, 1 layer)	2.541	0.61179	2.04E+00	2.41E-01
Plasterboard (5mm air gap, 2 layer)	2.1333	0.00299	9.98E-03	1.40E-03
Plasterboard	2.6	0.0364	1.21E-01	1.40E-02
Plasterboard	3.08	0.05544	1.85E-01	1.80E-02
Plasterboard (9mm)	2.37	0.12012	4.01E-01	5.07E-02
Plasterboard (12mm)	2.7	0.05346	1.78E-01	1.98E-02
Chipboard	2.78	0.1362	4.55E-01	4.90E-02
Chipboard	3.15	0.1795	5.99E-01	5.70E-02
Chipboard (22mm, wood)	2.85	0.15875	5.30E-01	5.57E-02
Thermolite block (100mm, 1 layer)	2.9396	0.2725	9.10E-01	9.27E-02
Thermolite block (100mm, 2 layer)	4.9913	0.32094	1.07E+00	6.43E-02
Ceiling board (8.8mm, rock wool)	1.5876	0.0126	4.21E-02	7.94E-03
Floor board (24.8mm, synthetic resin)	3.9135	0.32868	1.10E+00	8.40E-02
Stone	6.72	0.0336	1.12E-01	5.00E-03
Stone	8.55	0.5643	1.88E+00	6.60E-02
Marble	11.56	0.08092	2.70E-01	7.00E-03
Tiles	4.01	0.09223	3.08E-01	2.30E-02
Tiles	8.58	0.7807	2.61E+00	9.10E-02
Clear glass (4mm, 1 layer)	2.9591	0.00041	1.37E-03	1.38E-04
Clear glass (4mm, 2 layer)	6.3919	0.00032	1.07E-03	5.00E-05
Meshed glass (5mm, 1 layer)	8.0213	0.00024	8.01E-04	3.00E-05
Meshed glass (5mm, 2 layer)	3.4808	0.57364	1.91E+00	1.65E-01
Glass	4.7	0.1551	5.18E-01	3.30E-02
Glass	6.13	0.50266	1.68E+00	8.20E-02
Acrylic glass	2.52	0.03024	1.01E-01	1.20E-02
Plexiglas	2.76	0.018	6.01E-02	6.52E-03

4. WAVE PROPAGATION IN A DIELECTRIC LAYER

Consider a dielectric slab of thickness d, as illustrated in Figure 1. The problem of transmission and reflection of an incident wave can be treated as done for a Fabry-Perot etalon [7]-[8].

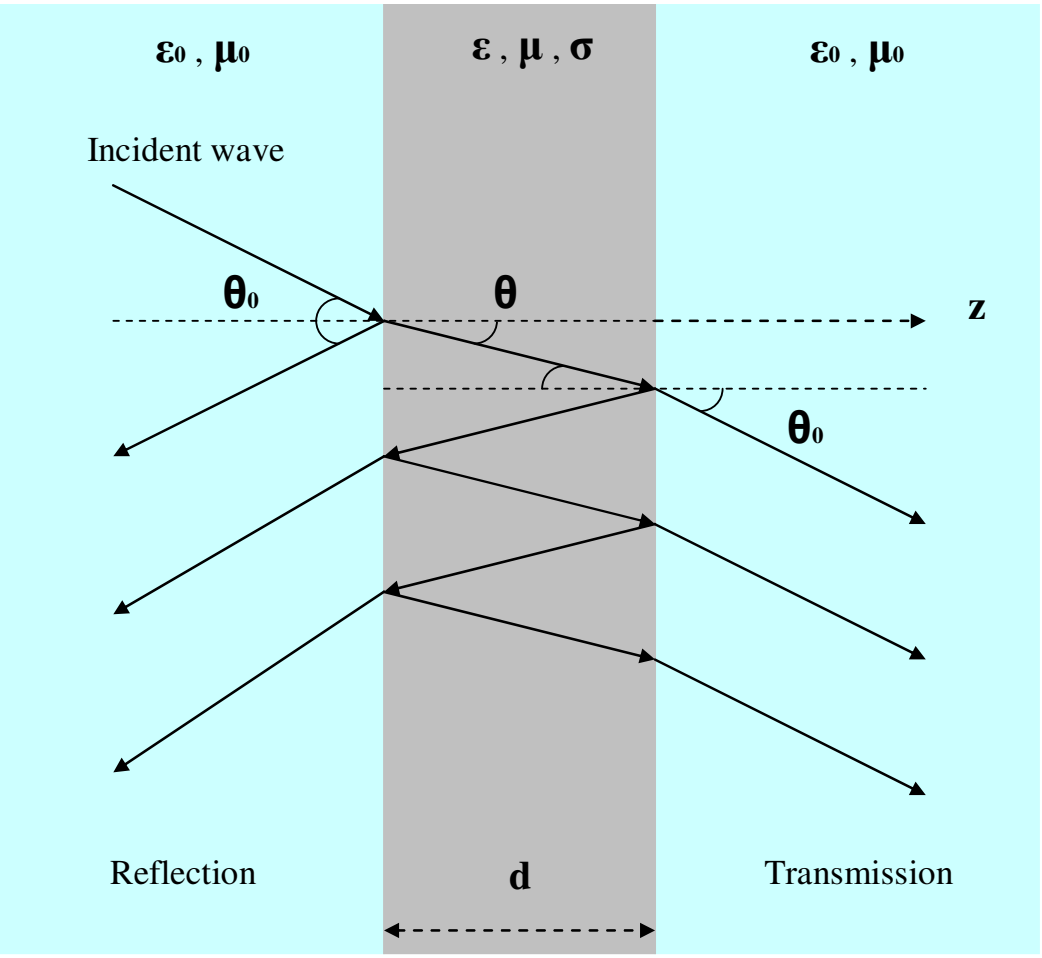

Figure 1: Wave propagation in a dielectric slab.

When the wave is incident at an angle θ relative to the normal of the interface between dissimilar media, the field reflection coefficient is given by [9]:

(13)
$$r = \rho_0 \left\{ 1 - \left[\left(1 - \rho_0^{\,2} \right) e^{-j2k_z(f)d} \right] \sum_{i=0}^{\infty} \left[\rho_0^{\,2} e^{-j2k_z(f)d} \right]^i \right\} =$$
$$= \rho_0 \cdot \frac{1 - e^{-j2k_z(f)d}}{1 - \rho_0^2 e^{-j2k_z(f)d}} = \rho_0 \cdot \frac{1 - e^{-2(\alpha + j\beta)\cos(\theta)d}}{1 - \rho_0^2 e^{-2(\alpha + j\beta)\cos(\theta)d}}$$

The coefficient ρ_0 is resulted from the Fresnel's equations [9]-[10]. When the electric field component of the wave is perpendicular to the plane of incidence (TE-wave):

(14)

$$\rho_{0-TE} = \frac{\cos(\theta_0) - \sqrt{\varepsilon_r - \sin^2(\theta_0)}}{\cos(\theta_0) + \sqrt{\varepsilon_r - \sin^2(\theta_0)}}$$

For the case of parallel polarization, where the incident electric field vector is in the plane of incidence (TM-wave):

(15)

$$\rho_{0-TM} = \frac{\sqrt{\varepsilon_r - \sin^2(\theta_0)} - \varepsilon_r \cos(\theta_0)}{\sqrt{\varepsilon_r - \sin^2(\theta_0)} + \varepsilon_r \cos(\theta_0)}$$

The field transmission of the electromagnetic wave through the slab is described by the expression:

(16)

$$t = \frac{\left(1-\rho_0^2\right)e^{-jk_z(f)d}}{1-\rho_0^2 e^{-j2k_z(f)d}} = \frac{\left(1-\rho_0^2\right)e^{-(\alpha+j\beta)\cos(\theta)d}}{1-\rho_0^2 e^{-2(\alpha+j\beta)\cos(\theta)d}}$$

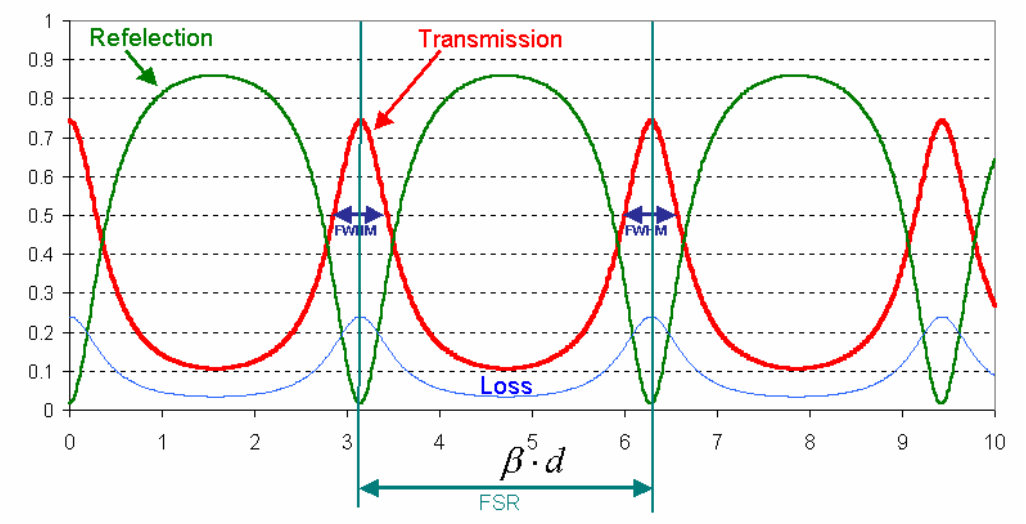

Figure 2: Reflection, Transmission and Loss in a dielectric slab.

The free spectral range (FSR) between transmission peaks is given for low loss materials (small imaginary dielectric constant) by:

(17)

$$FSR \cong \frac{c}{2d \cdot \sqrt{\varepsilon'(f)} \cdot \cos(\theta)} \cdot \left[1 + \frac{f}{2\varepsilon'(f)} \cdot \frac{d\varepsilon'(f)}{df}\right]^{-1}$$

The full width at half maximum (FWHM) of the transmission peaks is given by:

(18)

$$FWHM = \frac{FSR}{Finesse}$$

In which the Finesse is defined by:

(18)
$$Finesse = \frac{\pi\sqrt{|\rho_0|e^{-\alpha\cos(\theta)d}}}{1-|\rho_0|e^{-\alpha\cos(\theta)d}}$$

5. NUMERICAL RESULTS

The formulation described in the previous sections was used to evaluate field transmission and reflection coefficients of a concrete wall (Table 1 – concrete one year old) with a diffraction coefficient $n = \sqrt{\varepsilon'} = \sqrt{5.5}$. The Transmission coefficient at frequencies of 3-10 GHz and 0^0 incident angle is given in figure 3:

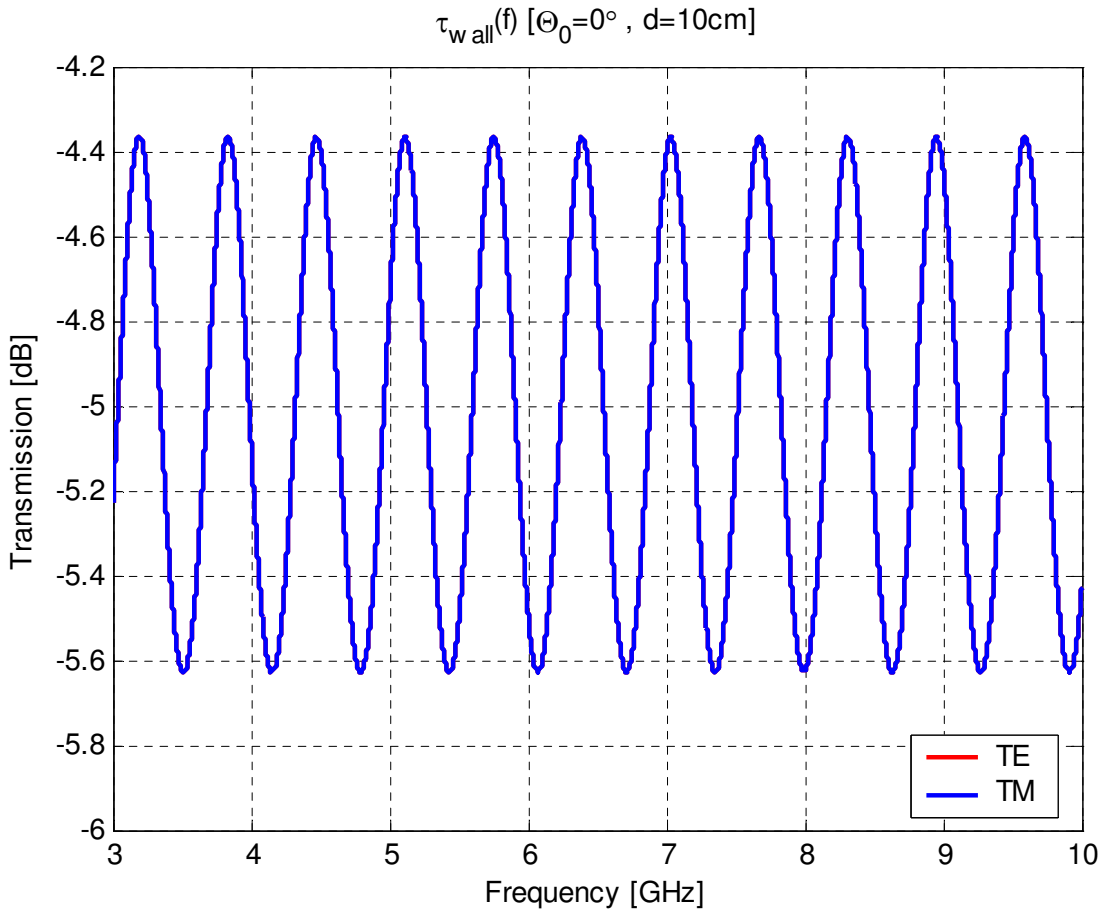

Figure 3: Transmission through a dielectric slab of one year old concrete.

The oscillatory nature of the transmission coefficient is evident and using equation (17) one arrives at the spectral range value:

(19)
$$FSR = \frac{1}{2}\frac{v_g}{d} \cong \frac{1}{2}\frac{c/n}{d} = \frac{1}{2}\frac{3\cdot 10^8}{\sqrt{5.5}\cdot 0.1} \approx 640MHz$$

Propagating a short pulse of 0.2 nano second duration through the same slab one obtains intriguing dispersion effects as is evident in figure 4. It seems that in addition to the "original pulse" one obtains a secondary pulse which can be attributed to a reflection from the far surface of the slab. Calculating the round trip propagation time of the signal in the slab on obtains:

(20)
$$t_r = \frac{2d}{v_g} \cong \frac{2d}{c/n} = \frac{2 \cdot 0.1}{3 \cdot 10^8 / \sqrt{5.5}} \approx 1.56nS$$

This can be compared with the temporal difference in both signals as is evident from the upper graph of figure 4. Such effects should be taken into account when designing the receiver of a communication signal.

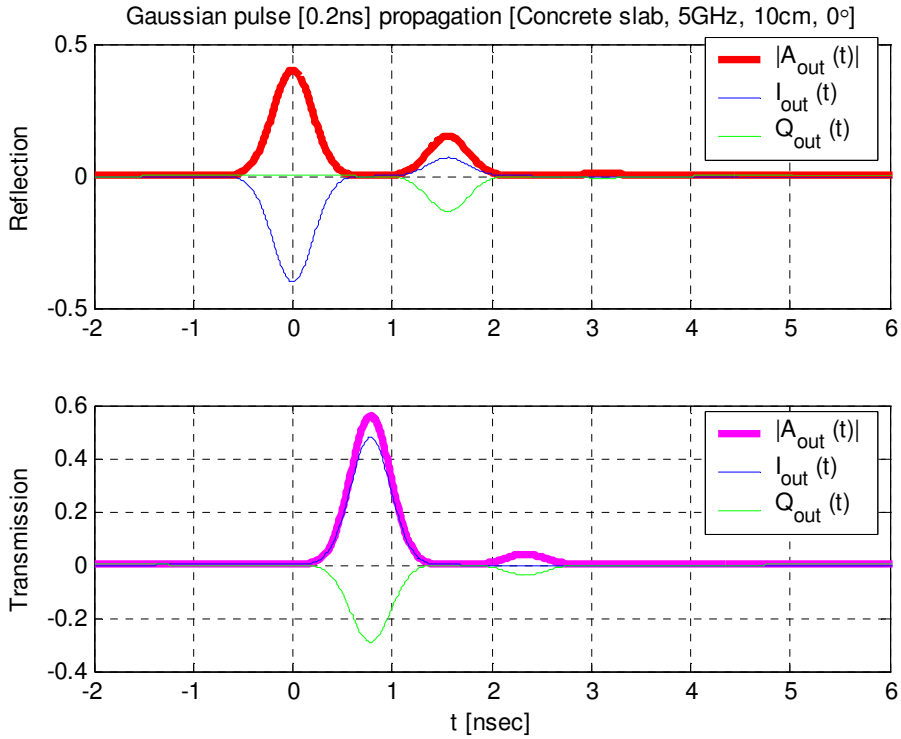

Figure 4: Short pulse through a dielectric slab of one year old concrete, Reflection & Transmission

6. ACKNOWLEDGEMENTS

The research was carried out in the framework of the Israeli Short Range Consortium, supported by the MAGNET program of the State of Israel Ministry of Industry and Commerce. We also acknowledge the help of Dr. David Behar from MICROKIM and useful discussions.

7. REFERENCES

1. P. Smulder: “Exploiting the 60GHz Band for local wireless multimedia access: prospects and future directions”, IEEE Communication Magazine, (January 2002), 140-147
2. IST-BROADWAY WP1-D2 deliverable: “Functional system parameters description”, (October 2002)
3. T. S. Rappaport, S. Sandhu: “Radio-wave propagation for emerging wireless personal communication systems”, IEEE Antenna an Propagation Magazine 36, (1994), 14-36
4. A. Safaai-Jazi, S. M. Riad, A. Muqaubel, A. Bayram: “Report on through –the-wall propagation and material characterization”, carried out in the framework of the DARPA NETEX program “Ultra-wideband propagation measurements and channel modeling”, (November 2002)
5. Y. Pinhasi, Yu. Lurie, A. Yahalom: “Space-frequency model of ultra wide-band interactions in millimeter wave masers”, Phys. Rev. E 71, (2005), 036503
6. P. Diament: “Wave transmission and fiber optics”, Maxwell Macmillan International Editions (1990)
7. C. Fabry, A. Perot: “Theorie et applications d’une nouvelle methode de spectroscopie interferentielle”, Ann. Chim. Phys., 16, (1899), 115
8. A. Yariv: “Quantum Electronics”, Wiley (1988)
9. H. J. Reed, T. S. Rappaport, B. D. Woerner: “Wireless Personal Communications: Advances in Coverage and Capacity”, Kluwer Academic Publishers (1997)
10. A. H. Cherin: “An Introduction to optical fibers”, McGraw Hill (1985)